

Switching Spinless and Spinful Topological Phases with Projective PT Symmetry


Y. X. Zhao^{1,2,*}, Cong Chen,³ Xian-Lei Sheng³, and Shengyuan A. Yang⁴

¹National Laboratory of Solid State Microstructures and Department of Physics, Nanjing University, Nanjing 210093, China

²Collaborative Innovation Center of Advanced Microstructures, Nanjing University, Nanjing 210093, China

³School of Physics, and Key Laboratory of Micro-nano Measurement-Manipulation and Physics, Beihang University, Beijing 100191, China

⁴Research Laboratory for Quantum Materials, Singapore University of Technology and Design, Singapore 487372, Singapore

 (Received 21 September 2020; revised 21 January 2021; accepted 7 April 2021; published 12 May 2021)

A fundamental dichotomous classification for all physical systems is according to whether they are spinless or spinful. This is especially crucial for the study of symmetry-protected topological phases, as the two classes have distinct symmetry algebra. As a prominent example, the spacetime inversion symmetry PT satisfies $(PT)^2 = \pm 1$ for spinless/spinful systems, and each class features unique topological phases. Here, we reveal a possibility to switch the two fundamental classes via \mathbb{Z}_2 projective representations. For PT symmetry, this occurs when P inverts the gauge transformation needed to recover the original \mathbb{Z}_2 gauge connections under P . As a result, we can achieve topological phases originally unique for spinful systems in a spinless system, and vice versa. We explicitly demonstrate the claimed mechanism with several concrete models, such as Kramers degenerate bands and Kramers Majorana boundary modes in spinless systems, and real topological phases in spinful systems. Possible experimental realization of these models is discussed. Our work breaks a fundamental limitation on topological phases and opens an unprecedented possibility to realize intriguing topological phases in previously impossible systems.

DOI: [10.1103/PhysRevLett.126.196402](https://doi.org/10.1103/PhysRevLett.126.196402)

Symmetry-protected topological phases have constituted one of the most active fields over the last decade and a half [1–6]. Based on mathematical tools such as the K and KO theories [7,8], rich topological phases have been proposed and classified by considering various internal and space group symmetries [9–16].

In this endeavor, a fundamental dichotomy is to distinguish systems based on whether they are spinful or spinless. For electronic systems, this corresponds to whether spin-orbit coupling (SOC) is included or not. The two categories exhibit distinct topological classifications. The reason is that for spinful systems, due to SOC, symmetry transformations must simultaneously act on both the orbital and the spin degrees of freedom, leading to symmetry algebra distinct from spinless systems.

A prominent example is the spacetime inversion symmetry PT . For spinful systems, $(PT)^2 = -1$, which dictates a Kramers double degeneracy at every k point in the Brillouin zone (BZ). In contrast, for spinless systems, $(PT)^2 = 1$, which instead guarantees a real band structure, because one can always choose a representation with $\hat{P}\hat{T} = \hat{K}$, with \hat{K} the complex conjugation. Each class hosts its own unique collection of topological phases [15]. For instance, PT -invariant spinful systems can realize 3D Dirac semimetals, 1D topological insulators or superconductors in class DIII; whereas spinless systems harbor real Dirac semimetals [17], \mathbb{Z}_2 -charged nodal surfaces [18], nodal-line linking structures [19–21], boundary phase

transitions [22], etc. [23–25]. A list of topological classification when including PT and sublattice symmetry S is presented in Table I.

The spin class therefore imposes a fundamental constraint on the possible topological phases that a system can realize. *It is possible to break this limitation?* Namely, is it possible to realize spinful (spinless) topological phases in spinless (spinful) systems?

In this Letter, we discover an approach to achieve this possibility. The essence of our proposal is that in the presence of gauge degrees of freedom, symmetries of a system will be *projectively* represented, which may completely change the fundamental algebraic structure of the symmetry group [26]. Particularly, we show that this can be achieved by coupling to a \mathbb{Z}_2 gauge field. Here, $\mathbb{Z}_2 = \{\pm 1\}$ is the subgroup of the electromagnetic gauge

TABLE I. Topological classification table for spacetime inversion and sublattice symmetries.

	$(PT)^2$	S	$d = 1$	$d = 2$	$d = 3$
AI	+	0	\mathbb{Z}_2	\mathbb{Z}_2	0
BDI	+	$[S, PT] = 0$	\mathbb{Z}_2	0	$2\mathbb{Z}$
CI	+	$\{S, PT\} = 0$	\mathbb{Z}	\mathbb{Z}_2	\mathbb{Z}_2
AII	–	0	0	0	0
CII	–	$[S, PT] = 0$	0	0	\mathbb{Z}
DIII	–	$\{S, PT\} = 0$	$2\mathbb{Z}$	0	0

group $U(1)$, and physically just corresponds to switching the *sign* of certain hopping amplitudes. Remarkably, we find that the projectively represented symmetry PT may satisfy $(PT)^2 = -1$ [$(PT)^2 = 1$] for spinless (spinful) systems, namely, that we can switch the fundamental symmetry algebras between spinless and spinful systems. In a sense, we hence effectively make a spinful system behave as a spinless one, and vice versa. We explicitly demonstrate our idea via several concrete models, such as Kramers degenerate bands and Kramers Majorana boundary modes in spinless systems, and real Stiefel-Whitney topological phases in spinful systems. Experimental realizations of these models are discussed.

Our work opens up an unprecedented possibility to switch the fundamental categories of topological systems and to achieve intriguing topological phases in previously impossible systems.

Projective PT symmetry.—Let us start with a general discussion of the PT symmetry. Ordinarily, for a system consisting of particles with spin s , the time-reversal symmetry satisfies $T^2 = (-1)^{2s}$, and the space inversion symmetry satisfies $P^2 = 1$. They commute with each other, $[P, T] = 0$, and, therefore,

$$(PT)^2 = (-1)^{2s}. \quad (1)$$

For instance, in the internal space of an electron (which is spinful), we have $(PT)^2 = -1$. The common textbook explanation is that T is represented by $\hat{T} = -i\sigma_2\hat{K}$ with $T^2 = -1$, while P is represented by $\hat{P} = \sigma_0$, which preserves the spin. Here, σ 's are the Pauli matrices for spin. On the other hand, for spinless particles, $\hat{T} = \hat{K}$ and $\hat{P} = 1$, and therefore $(PT)^2 = 1$.

However, in the presence of certain gauge degrees of freedom, the relation $(PT)^2 = (-1)^{2s}$ will be projectively represented, because the inversion is a spatial symmetry and may involve additional gauge transformations. Here, we request that the gauge flux configuration is invariant under P , i.e., P is still a symmetry of the system. Nevertheless, the chosen gauge connections do not necessarily preserve P . Then, to recover the gauge configuration, a gauge transformation \mathbf{G} must be incorporated into the inversion. Thus, the *proper* inversion actually becomes a combined operation,

$$\mathbf{P} = \mathbf{G}P. \quad (2)$$

Specifically, for a \mathbb{Z}_2 gauge theory, \mathbf{G} preserves T and $\mathbf{G}^2 = 1$. In addition, if P reverses the gauge transformations, i.e., \mathbf{G} anticommutes with P , then we have the following relations:

$$[\mathbf{G}, T] = 0, \quad \{\mathbf{G}, P\} = 0, \quad \mathbf{G}^2 = 1. \quad (3)$$

It follows that $\mathbf{P}^2 = (\mathbf{G}P)^2 = -1$. Thus, the *proper* space-time inversion symmetry \mathbf{PT} will satisfy a distinct algebra:

$$(\mathbf{PT})^2 = \mathbf{P}^2T^2 = (-1)^{2s+1}. \quad (4)$$

This is remarkable, because it shows that, with the help of \mathbb{Z}_2 gauge fields, the fundamental symmetry algebra can be exchanged for spinless and spinful systems. Consequently, their topological classifications are also exchanged. For instance, in the tenfold classification of Hamiltonian spaces, the topological phases of classes AI, BDI, and CI (AII, CII, and DIII) as shown in Table I can now be realized also by spinful (spinless) systems. Here, the tenfold classification involves the sublattice symmetry, but clearly, the discussion can be extended to other symmetries such as various crystalline symmetries as well.

Below, we present three concrete models to demonstrate our idea. More examples can be found in the Supplemental Material [27].

Kramers Majorana modes in a 1D spinless chain.—Our first example is a 1D spinless model which realizes a class DIII topological gapped phase originally unique for spinful systems (see Table I).

The model is illustrated in Fig. 1(a). The unit cell (indicated by the shaded cube) contains eight sites, indexed by three qubits, ρ , τ , and σ . The inversion operator flips all three qubits, therefore in momentum space is given by

$$\hat{P} = \Gamma_{111}\hat{I}, \quad (5)$$

where we define

$$\Gamma_{\mu\nu\lambda} = \rho_\mu \otimes \tau_\nu \otimes \sigma_\lambda, \quad (6)$$

with $\mu, \nu, \lambda = 0, 1, 2, 3$, and \hat{I} is the momentum inversion operator.

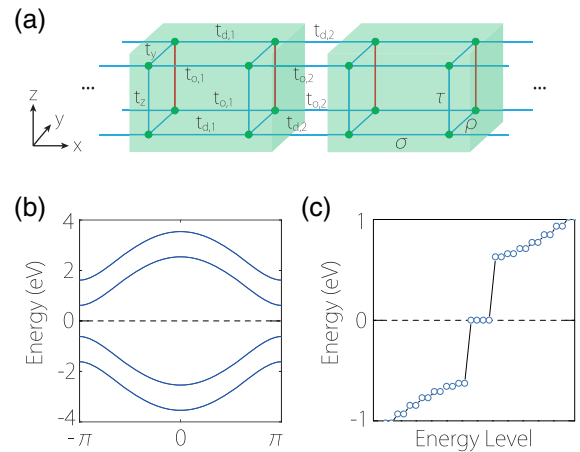


FIG. 1. (a) Schematic figure of the 1D spinless chain. Each unit cell (indicated by the green cubes) contain eight sites. The hopping amplitudes along x are marked in the figure. The red bonds have a negative hopping amplitude $-t_z$. (b) Calculated bulk band structure. Each band is twofold degenerate. (c) Spectrum of a finite chain with a length of 30 unit cells. The four zero modes form two Majorana Kramer pairs. Each pair is localized at one end of the chain.

The \mathbb{Z}_2 gauge field is specified that each plaquette normal to the x direction has a π flux, and all others have a zero flux. One gauge-connection configuration is shown in Fig. 1(a), where only each red-colored bond has negative sign in the hopping amplitude.

Clearly, the flux configuration respects the P symmetry, however, the gauge-connection configuration in Fig. 1(a) does not. To restore the original gauge configuration, the proper inversion \hat{P} should include the following gauge transformation:

$$\hat{G} = \Gamma_{003}, \quad (7)$$

which imposes a minus sign for sites on the bottom layer, and therefore, flips the sign for hopping amplitudes along z . Hence, the proper inversion operator is $\hat{P} = \hat{G} \hat{P} = i\Gamma_{112} \hat{T}$, and the spacetime inversion is represented by

$$\hat{P} \hat{T} = i\Gamma_{112} \hat{K}. \quad (8)$$

Importantly, note that P inverts the gauge transformation \hat{G} , such that $\{\hat{G}, \hat{P}\} = 0$. Therefore, according to our analysis above [see Eqs. (3) and (4)], the projective PT symmetry of this spinless chain follows a modified algebra $(PT)^2 = -1$, a character intrinsic to spinful systems.

With the hopping amplitudes shown in Fig. 1(a), the tight-binding model can be written as

$$\mathcal{H}(k) = t_y \Gamma_{010} + t_z \Gamma_{301} + \sum_{s=d,o} \begin{bmatrix} 0 & u_s(k) \\ u_s^*(k) & 0 \end{bmatrix} \otimes M_s. \quad (9)$$

Here, k is the momentum along x , $M_d = \text{diag}(1, 0, 0, 1)$, $M_o = \text{diag}(0, 1, 1, 0)$, and $u_s(k) = t_{s,1} + t_{s,2} e^{-ik}$.

The sublattice symmetry is represented as $\hat{S} = \Gamma_{333}$. It can be transformed into the standard form Γ_{300} by the unitary transformation $U = \exp[(i\pi/4)\Gamma_{100}] \exp[-(i\pi/4)\Gamma_{133}]$. Accordingly, the Hamiltonian can be converted into the standard block off-diagonal form as for class DIII systems

$$U \mathcal{H} U^\dagger = \begin{bmatrix} 0 & Q(k) \\ Q^\dagger(k) & 0 \end{bmatrix}. \quad (10)$$

For gapped phases in class DIII, the 1D topological invariant is given by the winding number

$$\nu = \frac{1}{2\pi i} \oint dk \text{tr} Q^{-1}(k) \partial_k Q(k). \quad (11)$$

This winding number is valued in even integers $2\mathbb{Z}$ due to the algebraic relations $(\hat{P} \hat{T})^2 = -1$ and $\{\hat{P} \hat{T}, \hat{S}\} = 0$, as proved in the Supplemental Material [27].

For instance, the system is nontrivial with $\nu = 2$, when we set $t_y = t_z = 0.5$, $t_{d,1} = t_{o,2} = 2$, and $t_{d,2} = t_{o,1} = 1$. The corresponding band bulk structure is shown in Fig. 1(b), showing a gapped spectrum. Note that although the system is spinless, each band here has a Kramers double degeneracy due to $(PT)^2 = -1$. The invariant $\nu = 2$ dictates that for a PT -symmetric chain with an open boundary condition, there must exist a Kramers pair of Majorana modes at each boundary, which is confirmed by our result in Fig. 1(c). Previously, such Kramers Majorana pair is only possible for spinful systems, such as the 1D T -invariant p -wave topological superconductor. Here, we demonstrate that it can be successfully extended to spinless systems via our proposed mechanism. Since only the nearest neighbor hopping is needed here, the topological phase could be easily realized by various artificial systems.

2D real Dirac semimetal in a spinful lattice.—In the second example, we achieve a 2D phase with real twofold Dirac points. The real Dirac point is previously unique for spinless systems. A famous example is graphene. It is protected by the first Stiefel-Whitney number ν_{1D} , which just corresponds to the quantized Berry phase along a circle. Here, we will realize it in a spinful system.

As illustrated in Fig. 2(a), the 2D model consists of two layers of square lattices. Each square plaquette normal to the y direction has a π flux. A possible gauge configuration is shown in Fig. 2(a), where the red-color bonds have a negative hopping amplitude. A unit cell contains four sites, which are labeled by two qubits ρ and τ [Fig. 2(a)], and the spin basis on each site is denoted by σ .

Clearly, the inversion $\hat{P} = \Gamma_{110} \hat{T}$ reverses the vertical hopping amplitudes, therefore the proper inversion must include a gauge transformation $\hat{G} = \Gamma_{300}$, which anti-commutes with \hat{P} . Hence, $\hat{P} = i\Gamma_{210} \hat{T}$. With the standard $\hat{T} = -i\Gamma_{002} \hat{T} \hat{K}$ for a spinful system, we obtain

$$\hat{P} \hat{T} = \Gamma_{212} \hat{K}, \quad (12)$$

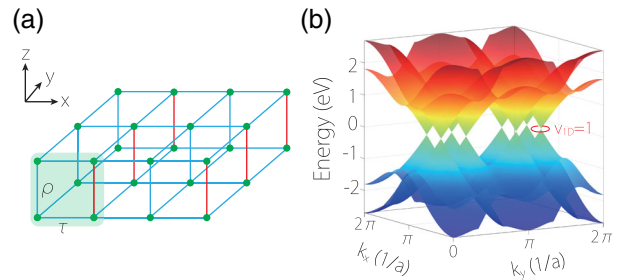


FIG. 2. (a) Schematic figure for the 2D model, consisting of two layers of square lattices. The unit cell consists of four sites as marked by the green square. The red colored bonds have a negative hopping amplitude $-t_z$. (b) Bulk band structure of the model (13). There are eight twofold real Dirac points at zero energy, protected by $\nu_{1D} = 1$. Here, we take parameters $t_x = t_y = t_z = 1$ and $\lambda = 0.5$.

which satisfies the identity $(\hat{P}\hat{T})^2 = 1$, so we have made the spinful system behave effectively as a spinless one.

With the hopping amplitudes specified in Fig. 2(a), our spinful lattice model is given by

$$\mathcal{H}(\mathbf{k}) = (t_x + t_x \cos k_x)\Gamma_{010} + t_x \sin k_x \Gamma_{020} + 2t_y \cos k_y \Gamma_{031} + t_z \Gamma_{130} + \lambda \Gamma_{303}. \quad (13)$$

Here, the third term is an explicit SOC term. Figure 2(b) shows a typical band structure for this model. The spectrum contains eight twofold Dirac points at zero energy. It is easy to verify that these are real Dirac points, each protected by a π Berry phase quantized by the projective PT symmetry.

This 2D real Dirac semimetal can be readily extended into a 3D real nodal-line semimetal by stacking its copies along the z direction, e.g., by adding the following vertical hopping terms to Eq. (13):

$$\mathcal{H}_z(k_z) = (t_z + t_z \cos k_z)\Gamma_{130} + t_z \sin k_z \Gamma_{230}. \quad (14)$$

They will generate four real nodal loops in the 3D BZ [27], and each loop is protected by a quantized π Berry phase.

Real Dirac point and doubly charged loop in generalized 3D Kane-Mele model.—The third example is a real topological phase characterized by the second Stiefel-Whitney number ν_{2D} , corresponding to class AI in Table I but realized in a spinful system.

Our model is constructed by stacking the renowned 2D Kane-Mele model with interlayer π fluxes. As shown in Fig. 3(a), the stacking forms a 3D graphite lattice, and the π flux only exists for each vertical rectangular plaquette. Figure 3(a) shows a possible gauge connection configuration, where again we use the red color to indicate the bonds with a negative hopping amplitude. We define a unit cell with four sites, as marked by the shaded region. These four sites are indexed by the qubits ρ and τ , and again the real spin is denoted by σ . Following similar analysis above, we find that the proper inversion operator \hat{P} must include $\hat{P} = \Gamma_{110}\hat{I}$ and the gauge transformation $\hat{G} = \Gamma_{300}$. Combined with $\hat{T} = -i\Gamma_{002}\hat{I}\hat{K}$ for spinful systems, we find $\hat{P}\hat{T} = \Gamma_{212}\hat{K}$, same as Eq. (12). Clearly, $(\hat{P}\hat{T})^2 = 1$, hence a spinful system is effectively turned into a spinless one.

The lattice model is given by

$$\mathcal{H}(\mathbf{k}) = \chi_1(\mathbf{k})\Gamma_{010} + \chi_2(\mathbf{k})\Gamma_{020} + \eta(\mathbf{k})\Gamma_{033} + \lambda_1(k_z)\Gamma_{130} + \lambda_2(k_z)\Gamma_{230}. \quad (15)$$

Here, $\chi_1 + i\chi_2 = t_1 \sum_{i=1}^3 e^{i\mathbf{k}\cdot\mathbf{a}_i}$, $\eta = -t_2 \sum_{i=1}^3 \sin \mathbf{k} \cdot \mathbf{b}_i$, where \mathbf{a}_i 's are the three bond vectors for the honeycomb lattice, and $\epsilon_{ijk}\mathbf{b}_k = \mathbf{a}_i - \mathbf{a}_j$ are the in-plane vectors between second neighbors. The first line is just the Kane-Mele model, and the η term is known as the intrinsic SOC term. The second line is the interlayer hopping, with $\lambda_1 + i\lambda_2 = J_1 + J_2 e^{ik_z}$.

Let us treat t_2 and $\delta J = J_2 - J_1$ as perturbations compared to t_1 and $J = (J_1 + J_2)/2$. When $t_2 = \delta J = 0$, there are two independent eightfold Fermi points at the corners of the BZ. Turning on t_2 and δJ , each Fermi point will split into two fourfold real Dirac points, each having a nontrivial second Stiefel-Whitney number $\nu_{2D} = 1$.

This Dirac semimetal actually represents a critical state, in the sense that it is unstable in the presence of other PT -invariant perturbations. However, due to the nontrivial ν_{2D} , the spectrum cannot be fully gapped. Instead, each Dirac point will evolve into a real nodal loop, protected by a twofold topological charge (ν_{1D}, ν_{2D}) (see Ref. [27] for more details, here, ν_{1D} is defined on a circle surrounding the loop). For example, consider adding to model (15) the following PT -invariant perturbations $\Delta\mathcal{H} = m_1\Gamma_{301} + m_2\Gamma_{302}$. The resulting doubly charged real loops are illustrated in Fig. 3(b).

Distinct from the usual nodal-loop semimetal in spinful systems, a hallmark of such a PT -invariant real nodal-loop semimetal is that it actually possesses a second-order topology; namely, it hosts protected hinge Fermi arcs.

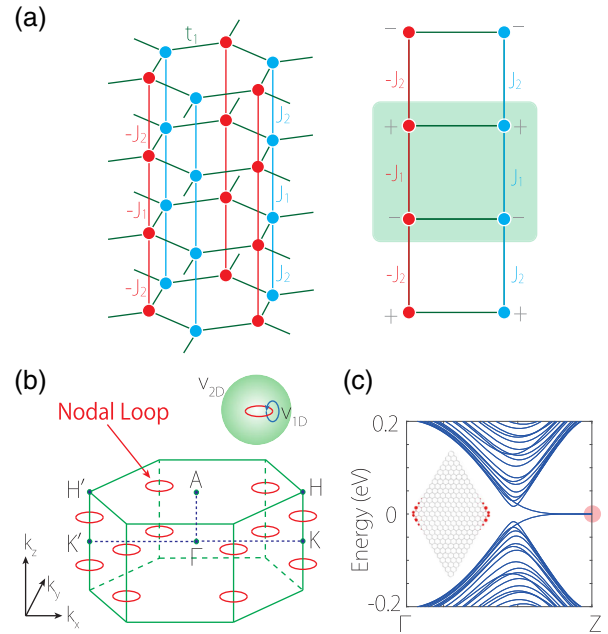


FIG. 3. (a) Schematic figure for the 3D generalized Kane-Mele model. Each 2D honeycomb layer is a 2D Kane-Mele model. The red colored bonds have negative hopping amplitudes $-J_1$ or $-J_2$. The unit cell contains four sites, as indicated by the shaded square in the right panel. (b) The bulk band structure contains four real nodal loops. Each loop is characterized by a twofold topological charge $(\nu_{1D}, \nu_{2D}) = (1, 1)$, as indicated by the inset. (c) Calculated spectrum of the system with a tubelike geometry extended along z and with a diamond-shaped cross section (see inset). The hinge Fermi arc states can be clearly visualized. Here, we take parameters $t_1 = 1$, $t_2 = 0.08$, $J_1 = 0.3$, $J_2 = 0.48$, $m_1 = 0.4$, and $m_2 = 0.3$.

This is explicitly confirmed by our numerical calculations, as shown in Fig. 3(c).

Discussion.—This work reveals an unprecedented possibility to break the fundamental limitation on topological phases by spin classes. We effectively switch the spin character of a system in terms of the symmetry algebra. Here, we focused on the PT symmetry. Clearly, the study can be extended to other symmetries and symmetry-protected topologies, which will open a new research field. The case of CP symmetry is briefly discussed in the Supplemental Material [27].

For interacting systems, the required \mathbb{Z}_2 gauge field can appear as remaining discrete gauge symmetry after symmetry breaking [33–35], or as emergent field in strongly correlated systems like spin liquids [36–41]. More importantly, it can be precisely engineered in artificial systems, such as photonic or phononic crystals, circuit networks, and mechanical periodic systems [28–32,42–50], which is briefly reviewed in the Supplemental Material [27]. Particularly, we suggest that the bright-dark mechanism, i.e., the effective hopping amplitude of two sites through an intermediate high-energy site is negative, could be a universal method to engineer \mathbb{Z}_2 gauge configurations for artificial systems [27].

The authors thank D. L. Deng for valuable discussions. This work is supported by National Natural Science Foundation of China (Grants No. 11874201 and No. 12074024), the Fundamental Research Funds for the Central Universities (Grant No. 14380119), and the Singapore Ministry of Education AcRF Tier 2 (MOE2017-T2-2-108).

*zhaoyx@nju.edu.cn

- [1] G. E. Volovik, *Universe in a Helium Droplet* (Oxford University Press, Oxford, 2003).
- [2] M. Z. Hasan and C. L. Kane, *Rev. Mod. Phys.* **82**, 3045 (2010).
- [3] X.-L. Qi and S.-C. Zhang, *Rev. Mod. Phys.* **83**, 1057 (2011).
- [4] S.-Q. Shen, *Topological Insulators* (Springer, Berlin, 2012).
- [5] A. Bansil, H. Lin, and T. Das, *Rev. Mod. Phys.* **88**, 021004 (2016).
- [6] N. P. Armitage, E. J. Mele, and A. Vishwanath, *Rev. Mod. Phys.* **90**, 015001 (2018).
- [7] M. F. Atiyah, *Q. J. Mech. Appl. Math.* **17**, 367 (1966).
- [8] M. Karoubi, *K-Theory: An Introduction* (Springer, New York, 1978).
- [9] P. Hořava, *Phys. Rev. Lett.* **95**, 016405 (2005).
- [10] A. P. Schnyder, S. Ryu, A. Furusaki, and A. W. W. Ludwig, *Phys. Rev. B* **78**, 195125 (2008).
- [11] A. Kitaev, *AIP Conf. Proc.* **1134**, 22 (2009).
- [12] Y. X. Zhao and Z. D. Wang, *Phys. Rev. Lett.* **110**, 240404 (2013).
- [13] Y. X. Zhao and Z. D. Wang, *Phys. Rev. B* **89**, 075111 (2014).
- [14] C.-K. Chiu, J. C. Y. Teo, A. P. Schnyder, and S. Ryu, *Rev. Mod. Phys.* **88**, 035005 (2016).
- [15] Y. X. Zhao, A. P. Schnyder, and Z. D. Wang, *Phys. Rev. Lett.* **116**, 156402 (2016).
- [16] J. Kruthoff, J. de Boer, J. van Wezel, C. L. Kane, and R.-J. Slager, *Phys. Rev. X* **7**, 041069 (2017).
- [17] Y. X. Zhao and Y. Lu, *Phys. Rev. Lett.* **118**, 056401 (2017).
- [18] W. Wu, Y. Liu, S. Li, C. Zhong, Z.-M. Yu, X.-L. Sheng, Y. X. Zhao, and S. A. Yang, *Phys. Rev. B* **97**, 115125 (2018).
- [19] T. Bzdušek and M. Sigrist, *Phys. Rev. B* **96**, 155105 (2017).
- [20] J. Ahn, D. Kim, Y. Kim, and B.-J. Yang, *Phys. Rev. Lett.* **121**, 106403 (2018).
- [21] Z. Wang, B. J. Wieder, J. Li, B. Yan, and B. A. Bernevig, *Phys. Rev. Lett.* **123**, 186401 (2019).
- [22] K. Wang, J.-X. Dai, L. B. Shao, S. A. Yang, and Y. X. Zhao, *Phys. Rev. Lett.* **125**, 126403 (2020).
- [23] J. Ahn, S. Park, and B.-J. Yang, *Phys. Rev. X* **9**, 021013 (2019).
- [24] X.-L. Sheng, C. Chen, H. Liu, Z. Chen, Z.-M. Yu, Y. X. Zhao, and S. A. Yang, *Phys. Rev. Lett.* **123**, 256402 (2019).
- [25] Q. Wu, A. A. Soluyanov, and T. Bzdušek, *Science* **365**, 1273 (2019).
- [26] G. W. Moore, Lecture notes: Abstract group theory (2020).
- [27] See Supplemental Material at <http://link.aps.org/supplemental/10.1103/PhysRevLett.126.196402> for (i) a brief review of \mathbb{Z}_2 gauge fields in artificial systems, (ii) the topological invariant for class DIII, (iii) technical details for the stacked Kane-Mele model, (iv) additional models, and (v) comments on switching topological superconductor classes, which includes Refs. [15,20,22,28–32].
- [28] S. Mittal, V. V. Orre, G. Zhu, M. A. Gorlach, A. Poddubny, and M. Hafezi, *Nat. Photonics* **13**, 692 (2019).
- [29] H. Xue, Y. Ge, H.-X. Sun, Q. Wang, D. Jia, Y.-J. Guan, S.-Q. Yuan, Y. Chong, and B. Zhang, *Nat. Commun.* **11**, 2442 (2020).
- [30] S. Imhof, C. Berger, F. Bayer, J. Brehm, L. W. Molenkamp, T. Kiessling, F. Schindler, C. H. Lee, M. Greiter, T. Neupert, and R. Thomale, *Nat. Phys.* **14**, 925 (2018).
- [31] R. Yu, Y. X. Zhao, and A. P. Schnyder, *Natl. Sci. Rev.* **7**, 1288 (2020).
- [32] E. Prodan and C. Prodan, *Phys. Rev. Lett.* **103**, 248101 (2009).
- [33] M. Sigrist and K. Ueda, *Rev. Mod. Phys.* **63**, 239 (1991).
- [34] F. Alexander Bais, P. van Driel, and M. de Wild Propitius, *Phys. Lett. B* **280**, 63 (1992).
- [35] L. M. Krauss and F. Wilczek, *Phys. Rev. Lett.* **62**, 1221 (1989).
- [36] G. Baskaran and P. W. Anderson, *Phys. Rev. B* **37**, 580 (1988).
- [37] X.-G. Wen, *Phys. Rev. B* **65**, 165113 (2002).
- [38] A. Kitaev, Special issue, *Ann. Phys. (Amsterdam)* **321**, 2 (2006).
- [39] X.-G. Wen, *Rev. Mod. Phys.* **89**, 041004 (2017).
- [40] Y. X. Zhao, Y. Lu, and S. A. Yang, arXiv:2005.14500.
- [41] E. H. Lieb, *Phys. Rev. Lett.* **73**, 2158 (1994).
- [42] D.-W. Zhang, Y.-Q. Zhu, Y. X. Zhao, H. Yan, and S.-L. Zhu, *Adv. Phys.* **67**, 253 (2018).
- [43] N. R. Cooper, J. Dalibard, and I. B. Spielman, *Rev. Mod. Phys.* **91**, 015005 (2019).
- [44] J. Dalibard, F. Gerbier, G. Juzeliūnas, and P. Öhberg, *Rev. Mod. Phys.* **83**, 1523 (2011).

- [45] N. Goldman, G. Juzeliūnas, P. Öhberg, and I. B. Spielman, *Rep. Prog. Phys.* **77**, 126401 (2014).
- [46] T. Ozawa, H.M. Price, A. Amo, N. Goldman, M. Hafezi, L. Lu, M. C. Rechtsman, D. Schuster, J. Simon, O. Zilberberg, and I. Carusotto, *Rev. Mod. Phys.* **91**, 015006 (2019).
- [47] G. Ma, M. Xiao, and C. T. Chan, *Nat. Rev. Phys.* **1**, 281 (2019).
- [48] L. Lu, J. D. Joannopoulos, and M. Soljai, *Nat. Photonics* **8**, 821 (2014).
- [49] Z. Yang, F. Gao, X. Shi, X. Lin, Z. Gao, Y. Chong, and B. Zhang, *Phys. Rev. Lett.* **114**, 114301 (2015).
- [50] S. D. Huber, *Nat. Phys.* **12**, 621 (2016).